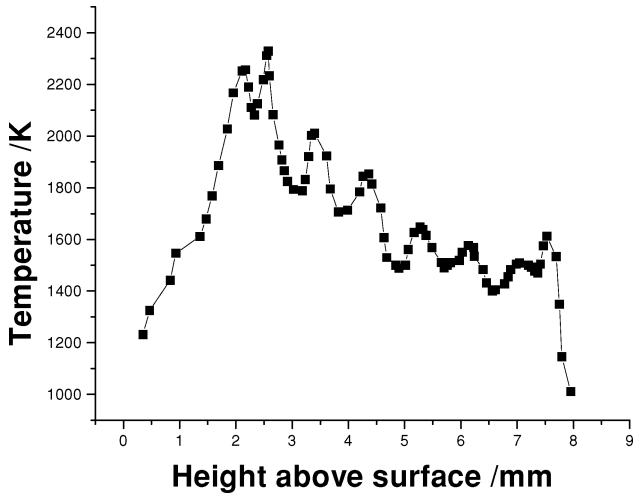

Fig. 3 Temperature distribution for NEPE propellant by spectroscopy method at 3-MPa pressure.

and the maximum time resolution for the temperature measurement of one point is about 10 μs, which is much smaller than the burning duration of SQ-2 propellant samples.

Conclusions

All results in this paper are given based on the following assumptions: 1) combustion of the flame is steady; 2) the flame is optically thin for its small size; and 3) the flame is in local thermal equilibrium state.

The temperature distributions in the axes for the SQ-2 propellant at different pressures are shown in Fig. 2. There are three areas, the climbing-temperature area, the high-temperature area and the fall-temperature area, in the temperature distribution. The temperature in the high-temperature area is unstable because of the turbulence of the flame and the unsteady of combustion. And also, this instability can be found in the line intensity data without Abel's inversion.

The maximum flame temperatures are compared with the results from thermocouple method and equilibrium calculation (shown in Table 1). The data of thermocouple method and equilibrium calculation are provided by the Beijing Institute of Technology.

The data in Table 1 show that the maximum flame temperature increases along with the rising of the pressure. The results from the spectroscopy method are about 100 K higher than those from the thermocouple method and much nearer to the temperature from equilibrium calculation with the rising of the pressure. As a reference, Dong Yang[1] has reported that the maximum temperatures of SQ-2 propellant exhaust plumes are 2234 and 2202 K for 240 and 500 mm apart from the motor nozzle when the work pressure of the chamber is about 13.0 MPa. The results from the spectroscopic diagnostic system are reasonable in comparison with the preceding results from other methods. The relative standard deviations of maximum temperature of the SQ-2 propellant's flame at different pressures are less than 5% for all measurements.

The temperature distribution of the solid-propellant nitrate-ester-plasticized polyethane (NEPE) is also measured by the spectroscopic diagnostic system. The result is not satisfactory because there are metal particles in the NEPE propellant, which will absorb and scatter the radiation, and emit their own spectrum. Figure 3 shows one of the measurement results. In fact, the temperature measurements for the NEPE propellant at different pressures are made for many times. The relative standard deviations of the maximum flame temperature are about 15% in our measurements, which are a little bit larger. This will be studied in the later work.

Acknowledgments

This research is supported by Beijing Institute of Technology. The first author thanks Jie Zhang and Yunfei Liu for their data of thermocouple method and equilibrium calculation.

References

[1]Yang, D., Xu, H. Q., Wang, J. D., and Zhao, B. C, "Temperature Measurement of Solid Rocket Motor Exhaust Plume by Absorption-Emission Spectroscopy," *Spectroscopy Letters*, Vol. 34, No. 2, 2001, pp. 109–116.

[2]Mallery, C. F., and Thynell, S. T., "Species and Temperature Profiles of Propellant Flames Obtained from FTIR Absorption Spectroscopy," *Combustion Science and Technology*, Vol. 122, No. 1–6, 1997, pp. 113–129.

[3]Wormhoudt, J., Kebabian, P. L., and Kolb, C. E., "Infrared Fiber-Optic Diagnostic Observations of Solid Propellant Combustion," *Combustion and Flame*, Vol. 108, No. 1–2, 1997, pp. 43–60.

[4]Zenin, A. A., and Finyarkov, S. V., "Study of Solid-Propellant Ignition by a Hot Gas-Stream," *Combustion Explosion and Shock Waves*, Vol. 29, No. 3, 1993, pp. 270–275.

[5]Zhao, W., Zhu, S., Tian, K., and Liu, D., "Quick Spectroscopy Diagnostics for the Flame Temperature," *Combustion of Energetic Materials*, edited by K. K. Kuo and L. T. Deluco, Begell House, New York, 2002, pp. 753–761.

[6]Venugopalan, M. (ed.), *Reactions Under Plasma Conditions*, Vol. 1, Wiley, New York, 1971, p. 389.

[7]Venugopalan, M. (ed.), *Reactions Under Plasma Conditions*, Vol. 1, Wiley, New York, 1971, p. 105.

[8]Kasabov, G. A., and Eliseev, V. V., *Spectrum Table for Low Temperature Plasma*, Moscow Atomic Energy Press, Moscow, 1973, pp. 160, 161.

Thermally Asymmetric Annular Rectangular Fin Optimization

H. S. Kang*
Kangwon National University, Chunchon 200-701, Republic of Korea
and
D. C. Look Jr.†
University of Missouri–Rolla, Rolla, Missouri 65409-0050

Nomenclature

Bi	=	Biot number, hl'/k
h_j	=	heat transfer coefficient of surface j, W/m^2 K
k	=	thermal conductivity of fin material, W/m K
l'	=	one-half fin height at the base, m; dimensionless form, $l = l'/r'_i$
M_j	=	convection characteristic number of surface j, $h_j r'_i/k (= B_{j1}/l)$
q	=	heat transfer from the fin, W; dimensionless form, $Q = q/k\varphi_f(2\pi r'_i)$
r'	=	radius, m; dimensionless form, $r = r'/r'_i$
r'_i	=	pipe inside radius, m
r'_j	=	j radius, m; dimensionless form, $r_j = r'_j/r'_i$

Received 3 September 2003; revision received 11 December 2003; accepted for publication 11 December 2003.

*Associate Professor, Department of Mechanical Engineering; hkang1960@yahoo.com.

†Professor Emeritus, Department of Mechanical and Aerospace Engineering and Engineering Mechanics; look@umr.edu. Associate Fellow AIAA.

T = two-dimensional temperature within the fin, K
T_b = fin base (root) temperature, K
T_f = fluid temperature inside pipe, K
T_∞ = surrounding temperature, K
V' = fin volume, m^3; dimensionless form, $V = V'/\pi r_i'^3$
z' = vertical coordinate, m; dimensionless form, $z = z'/r_i'$
α = bottom-to-top convection characteristic number ratio, M_2/M_1
β = tip-to-top convection characteristic number ratio, M_e/M_1
θ = dimensionless temperature, $(T - T_\infty)/(T_f - T_\infty)$
λ_n = eigenvalues, $n = 1, 2, 3, \ldots$
φ_f = modified fluid temperature, $(T_f - T_\infty)$, K

Subscripts

b = fin base (root)
e = fin tip
f = fluid inside pipe
1 = fin top
2 = fin bottom
∞ = surrounding

Superscript

$*$ = optimum

Introduction

EXTENDED surfaces have been used to enhance the rate of heat transfer from a primary surface to its surrounding fluid in many applications, such as air conditioning, the cooling of combustion engines or electronic components, and cryogenics. Annular fins, for example, are one of the important components of finned-tube heat exchangers and the optimization procedures for these fins have been an important concern for a long time.

The studies of the optimum dimensions for annular fins of various profiles have yielded several publications.[1–7] Brown[1] considered rectangular fins, whereas Mikk[2] investigated both rectangular and triangular fins. Ullmann and Kalman[3] analyzed four different profiles (rectangular, triangular, parabolic, and hyperbolic). Razelos and Imre[4] examined rectangular, triangular, and trapezoidal annular fins with variable thermal-conductivity and heat-transfer coefficients. Recently, Laor and Kalman[5] studied rectangular, triangular, and parabolic profiles, whereas Zubair et al.[6] presented a variable profile that can be reduced to a rectangular profile. These studies are based on a one-dimensional analysis. However, two-dimensional analysis, which shows the temperature distribution along the fin height, can be applied to a wide variety of sizes and shapes with accuracy (e.g., for a larger Biot number or for a fin that is relatively thick). Also, two-dimensional studies of annular fins have been published. Razelos and Georgiou[7] presented the variation of a removal number N_r (defined as a measure of heat transfer augmentation) as a function of $Bi^{1/2}$ for annular fins with constant thickness as well as triangular, parabolic profiles. Lalot et al.[8] presented an expression for the efficiency of annular fins made of two materials. Look[9] showed the heat-loss ratio between a fin and a bare pipe for a radial fin of uniform thickness using one- and two-dimensional methods. An interesting paper by Yovanovich et al.[10] has an analysis of thermally symmetric annular fins. The pertinent results are presented in the form of efficiency versus Biot number. These papers focus on the performance and fin height at the base, which is fixed. It appears, at this point, that information on an optimum design for thermally asymmetric annular fins appears to be lacking in the literature.

The purpose of this presentation is to examine the optimum steady-state design for vertical convective annular fins using two-dimensional analysis. This Note is based on the following assumptions: 1) heat transfer from the fluid to the inside radius of the pipe is equal to heat transfer through the fin base (the fin base temperature is not constant), 2) the fin tip is not insulated, losing heat by convection, and 3) the fin-top convection characteristic number is different from the fin-bottom convection characteristic number (thermal asymmetry).

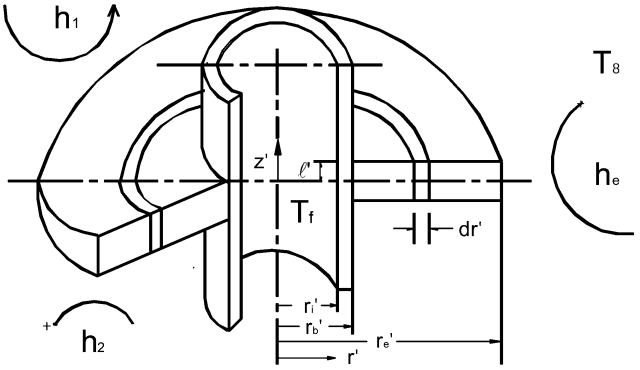

Fig. 1 Schematic of a thermally asymmetric annular rectangular fin.

Two-Dimensional Analysis

The nondimensional form of the governing equation for a thermally asymmetric annular rectangular fin, as illustrated in Fig. 1, can be written as

$$\frac{\partial^2\theta}{\partial r^2} + \frac{1}{r}\frac{\partial\theta}{\partial r} + \frac{\partial^2\theta}{\partial z^2} = 0 \tag{1}$$

The corresponding boundary conditions are shown as

$$-\left.\frac{\partial\theta}{\partial r}\right|_{r=r_b} = \frac{1-\theta|_{r=r_b}}{r_b/M_f + r_b\,\ell n(r_b)} \tag{2}$$

$$\left.\frac{\partial\theta}{\partial r}\right|_{r=r_e} + M_e\cdot\theta|_{r=r_e} = 0 \tag{3}$$

$$\left.\frac{\partial\theta}{\partial z}\right|_{z=l} + M_1\cdot\theta|_{z=l} = 0 \tag{4}$$

$$\left.\frac{\partial\theta}{\partial z}\right|_{z=-l} - M_2\cdot\theta|_{z=-l} = 0 \tag{5}$$

The solution $\theta(r, z)$ within the fin is presented by Eqs. (6–15):

$$\theta(r,z) = \sum_{n=1}^{\infty} N_n\cdot f(r)\cdot f(z) \tag{6}$$

where

$$f(r) = I_0(\lambda_n r) + f_n K_0(\lambda_n r) \tag{7}$$

$$f(z) = \cos(\lambda_n z) + g_n\sin(\lambda_n z) \tag{8}$$

$$N_n = \frac{4\cdot\sin(\lambda_n l)}{A_n}\frac{1}{B_n + C_n} \tag{9}$$

$$A_n = [2\lambda_n l + \sin(2\lambda_n l)] + g_n^2[2\lambda_n l - \sin(2\lambda_n l)] \tag{10}$$

$$B_n = I_0(\lambda_n r_b) + f_n K_0(\lambda_n r_b) \tag{11}$$

$$C_n = \lambda_n\left[\frac{r_b}{M_f} + r_b\,\ell n(r_b)\right][f_n K_1(\lambda_n r_b) - I_1(\lambda_n r_b)] \tag{12}$$

$$f_n = \frac{\lambda_n I_1(\lambda_n r_e) + M_e I_0(\lambda_n r_e)}{\lambda_n K_1(\lambda_n r_e) - M_e K_0(\lambda_n r_e)} \tag{13}$$

$$g_n = \frac{\lambda_n\sin(\lambda_n l) - M_1\cos(\lambda_n l)}{\lambda_n\cos(\lambda_n l) + M_1\sin(\lambda_n l)} \tag{14}$$

$$= \frac{M_2\cos(\lambda_n l) - \lambda_n\sin(\lambda_n l)}{\lambda_n\cos(\lambda_n l) + M_2\sin(\lambda_n l)} \tag{15}$$

The eigenvalues are calculated using Eqs. (14) and (15). The heat loss is calculated as indicated by

$$q = \int_{-l'}^{l'} -k\frac{\partial T}{\partial r'}\bigg|_{r'=r_b'} 2\pi r_b'\,\mathrm{d}z' = -k\varphi_f(2\pi r_i')\int_{-l}^{l}\frac{\partial\theta}{\partial r}\bigg|_{r=r_b} r_b\,\mathrm{d}z \tag{16}$$

Further, the dimensionless form of the heat loss can be expressed as

$$Q = \frac{q}{k\varphi_f(2\pi r_i')} = -2\sum_{n=1}^{\infty} N_n H_n r_b \sin(\lambda_n l) \tag{17}$$

where

$$H_n = I_1(\lambda_n r_b) - f_n K_1(\lambda_n r_b) \tag{18}$$

Finally the fin volume is calculated by

$$V' = 2\int_{r_b'}^{r_e'} 2\pi r' l'\,\mathrm{d}r' = 4\pi r_i'^3\int_{r_b}^{r_e} rl\,\mathrm{d}r \tag{19}$$

The dimensionless form of the fin volume is

$$V = V'\big/\pi r_i'^3 = 2l\left(r_e^2 - r_b^2\right) \tag{20}$$

Results

The results presented here were calculated for only a few typical values of the pertinent parameters, including a constant fin volume in most cases. The dimensionless temperature profiles along the fin-tip height are presented as Fig. 2 in the case of convection characteristic number ratios of $\alpha = 0.8$, 0.9, and 1. As expected, the temperature profile for $\alpha = 1$ is symmetric, whereas the temperature at the top surface is lower than the temperature at the bottom surface for $\alpha = 0.8$ and 0.9. The figure also indicates that temperature decreases as α increases at the same z-coordinate position; this statement is based on the fact that the average of all of the surface convection characteristic numbers increases as α increases.

Table 1 lists the dimensionless temperature at the fin base with the variation of fin-base radius, tip radius, fin-top-surface convection characteristic number, and convection characteristic number inside the pipe in the case of $\alpha = 0.9$, $\beta = 1$, and $l = 0.1$. This table illustrates that the base temperature decreases as the fin base radius, tip radius, and top-surface convection characteristic numbers increase or the convection characteristic number inside the pipe decreases.

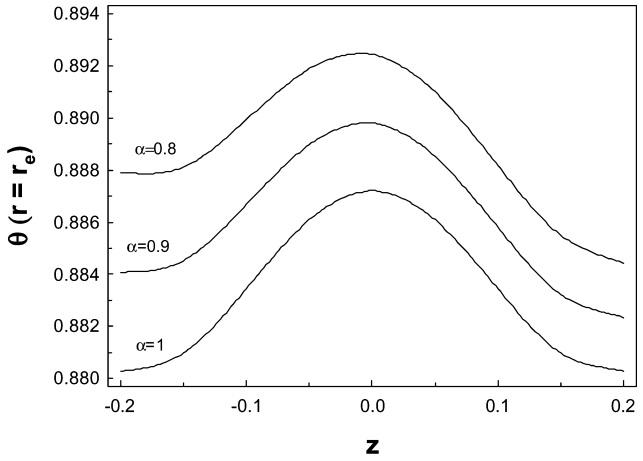

Fig. 2 Dimensionless temperature distribution along the fin-tip height with $M_1 = 0.1$, $\beta = 1$, $r_b = 1.1$, $r_e = 1.5$, $l = 0.2$, and $M_f = 1000$.

Table 1 Dimensionless base temperature with variations of r_b, r_e, M_f, and M_1 ($\alpha = 0.9$, $\beta = 1$, $l = 0.1$)

			$\theta(r = r_b, z = 0)$			
M_1	M_f	r_e	$r_b = 1.01$	$r_b = 1.05$	$r_b = 1.1$	$r_b = 1.2$
0.1	10	1.5	0.9337	0.9153	0.8970	0.8751
		2	0.8949	0.8623	0.8263	0.7684
	1000	1.5	0.9930	0.9700	0.9464	0.9152
		2	0.9884	0.9493	0.9061	0.8364
0.2	10	1.5	0.8871	0.8560	0.8251	0.7868
		2	0.8469	0.8007	0.7504	0.6701
	1000	1.5	0.9875	0.9467	0.9054	0.8504
		2	0.9823	0.9232	0.8591	0.7578

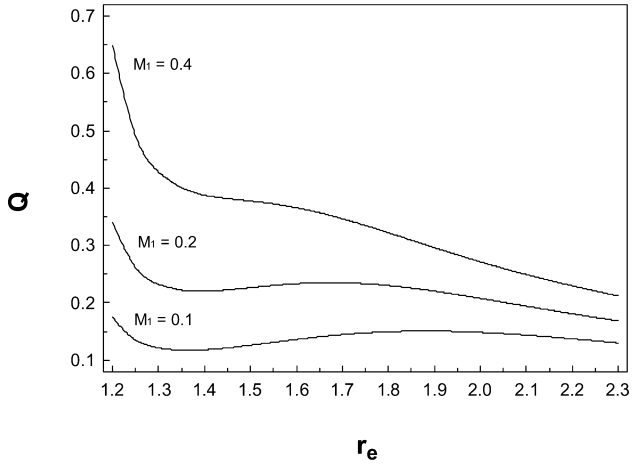

Fig. 3 Dimensionless heat loss as a function of fin tip radius for a fixed fin volume with $V = 0.3$, with $\alpha = 0.9$, $\beta = 1$, $r_b = 1.1$, and $M_f = 1000$.

It can be deduced that the fin base temperature approaches the fluid temperature inside the pipe as r_b approaches 1 and M_f approaches infinity for small values of fin-tip convection characteristic number and fin-tip radius. It also can be noted the base temperature for $r_e = 2$ decreases more rapidly than that for $r_e = 1.5$ as r_b increases. The arbitrarily selected values of $r_b = 1.1$ and $M_f = 1000$ will be used in all further discussions.

The constant-fin-volume dimensionless heat loss Q as a function of fin tip radius r_e is shown in Fig. 3. It appears that Q becomes unbounded when r_e approaches 1.2 (i.e., for an extremely short fin). The reason for this phenomenon can be explained physically as follows: because the fin volume V is constant, l^*, which represents the fin half-thickness at the fin base, will increase while r_e decreases. In other words, the extremely large Q is caused by increasing the half fin-base thickness l^*. Obviously, the design in this case is not practical. Another important phenomenon shown in Fig. 3 is that a maximum heat loss Q^* may not be always exist. That is, for $M_1 \leq 0.2$, the maximum heat loss will occur. In the case of $M_1 = 0.4$, it is seen that there is no maximum heat loss in the practical range of fin lengths. Therefore the optimum fin design is not obtainable when M_1 is beyond certain values.

Figure 4 presents the variation of the optimum heat loss. Q^* is the maximum nondimensional heat loss in the practical range of fin lengths and dimensions as a function of a for an annular fin of rectangular profile when the fin volume is fixed. This figure indicates that the optimum heat loss and the optimum fin half-thickness increase linearly, whereas the optimum fin-tip radius decreases linearly as a increases for three fin-base radii. Note that the optimum heat loss increases as the fin-base radius and the optimum fin half-thickness increase as the fin-base radius increases for a fixed value of a.

The effects of the Biot number ratio β on the optimum rectangular profile annular fin design under thermally asymmetric condition are shown as Fig. 5. The increase of β causes a slight increase

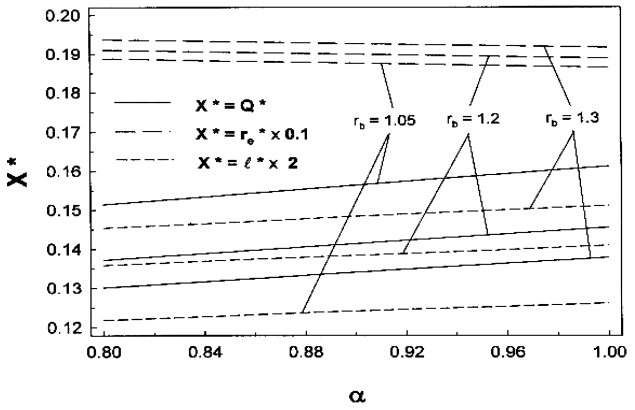

Fig. 4 Optimum heat loss vs α for $M_1 = 0.1$, $\beta = 1$, $V = 0.3$, and $M_f = 1000$.

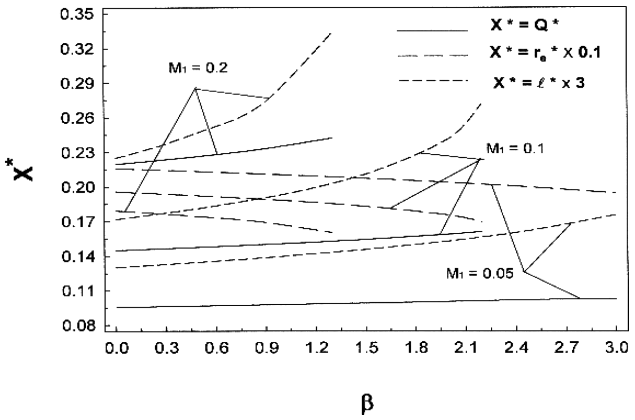

Fig. 5 Optimum heat loss vs β with $r_b = 1.1$, $\alpha = 0.9$, $V = 0.3$, and $M_f = 1000$.

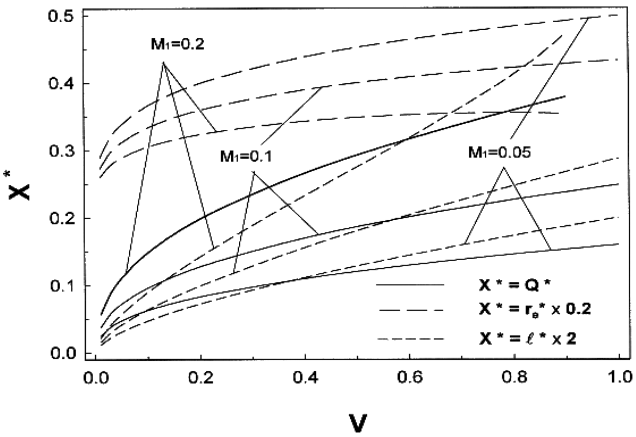

Fig. 6 Optimum heat loss V with $\alpha = 0.9$, $\beta = 1$, $r_b = 1.1$, and $M_f = 1000$.

of Q^* for the small values of M_1 and the effect of β on Q^* increases as M_1 increases. However, β has a relatively large influence on the optimum dimensions. For example, under a weak convection condition (i.e., $M_1 = 0.05$) when β increases from 0 to 3, the optimum fin-tip radius r_e^* decreases from 2.16 to 1.94, and the optimum half-fin base thickness l^* increases from 0.043 to 0.059 if we note that r_e^* is scaled 0.1 times smaller and l^* is scaled three times larger in this figure. Physically, a larger β represents stronger convection at the fin's top and bottom surface areas, or a shorter optimal fin-tip radius r_e^* is required. For the case of a fixed volume, l^* increases as r_e^* decreases, as shown in Fig. 5. The computations also reveal that the range of optimum designs decreases as M_1 increases, because the peak in the heat transfer does not exist there.

The variations of Q^* and optimum dimensions as a function of V under thermally asymmetric conditions are shown in Fig. 6. As expected, the increase of V enhances the optimum heat loss. That is, the optimum heat loss increases remarkably with respect to the fin volume; the rate of increase accelerates as M_1 becomes larger. The same trend is true for the optimum fin-tip radius, r_e^*. Finally, r_e^* increases rapidly at first and then levels off as V increases. It can be seen that r_e^* increases as M_1 decreases for the same fixed fin volume. Also, the optimum half fin-base thickness, l^*, increases almost linearly with the increase of total fin volume. Physically, the optimum annular fins of rectangular profile become fatter and longer with the increase of the fin volume, especially for a range of small values of V.

Conclusions

The optimum design of a single annular rectangular fin under thermally asymmetric conditions using a two-dimensional analysis has been presented. The influence of different parameters, such as the fin volume, the ratio of the fin-bottom convection characteristic number to the top convection characteristic number (α), and the ratio of the fin-tip convection characteristic number to the top convection characteristic number (β), to the optimum designs are discussed. This study shows that the optimum fin design is not obtainable when some parameters are beyond certain values. In the range where the maximum heat loss exists, both the optimum heat loss and the fin height increase and the optimum fin-tip radius decreases as α increases, or β increases, for a fixed volume. The optimum heat loss, fin length, and fin height increase as the fin volume increases when other variables are fixed.

References

[1]Brown, A., "Optimum Dimensions of Uniform Annular Fins," *International Journal of Heat and Mass Transfer*, Vol. 8, No. 4, 1965, pp. 655–662.

[2]Mikk, I., "Convective Fin of Minimum Mass," *International Journal of Heat and Mass Transfer*, Vol. 23, No. 5, 1980, pp. 707–711.

[3]Ullmann, A., and Kalman, H., "Efficiency and Optimized Dimensions of Annular Fin of Different Cross-Section Shapes," *International Journal of Heat and Mass Transfer*, Vol. 32, No. 6, 1989, pp. 1105–1110.

[4]Razelos, P., and Imre, K., "The Optimum Dimensions of Circular Fin with Variable Thermal Parameters," *Journal of Heat Transfer*, Vol. 102, No. 3, 1980, pp. 420–425.

[5]Laor, K., and Kalman, H., "Performance and Optimum Dimensions of Different Cooling Fins with a Temperature-Dependent Heat Transfer Coefficient," *International Journal of Heat and Mass Transfer*, Vol. 39, No. 9, 1996, pp. 1993–2003.

[6]Zubair, S. M., Al-Garni, A. Z., and Nizami, J. S., "The Optimal Dimensions of Circular Fins with Variable Profile and Temperature-Dependent Thermal Conductivity," *International Journal of Heat and Mass Transfer*, Vol. 39, No. 16, 1996, pp. 3431–3439.

[7]Razelos, P., and Georgiou, E., "Two-Dimensional Effects and Design Criteria for Convective Extended Surfaces," *Heat Transfer Engineering*, Vol. 13, No. 3, 1992, pp. 38–48.

[8]Lalot, S., Tournier, C., and Jensen, M., "Fin Efficiency of Annular Fins Made of Two Materials," *International Journal of Heat and Mass Transfer*, Vol. 42, No. 18, 1999, pp. 3461–3467.

[9]Look, D. C., Jr., "Fin on a Pipe (Insulated Tip): Minimum Conditions for Fin to Be Beneficial," *Heat Transfer Engineering*, Vol. 16, No. 3, 1995, pp. 65–75.

[10]Yovanovich, M. M., Culham, J. R., and Lemczyk, T. F., "Simplified Analytical Solutions to Circular Annular Fins with Contact Resistance and End Cooling," *Journal of Thermophysics and Heat Transfer*, Vol. 2, No. 2, 1988, pp. 152–157.